JBC Papers in Press. Published on August 3, 2017 as Manuscript M117.791269
The latest version is at http://www.jbc.org/cgi/doi/10.1074/jbc.M117.791269

Identification and Characterization of a Bacterial Cytochrome P450 Monooxygenase Catalyzing the 3-Nitration of Tyrosine in Rufomycin Biosynthesis

Hiroya Tomita[1,2], Yohei Katsuyama[1,2], Hiromichi Minami[3], and Yasuo Ohnishi[1,2]

[1]Department of Biotechnology, Graduate School of Agricultural and Life Sciences, The University of Tokyo, Bunkyo-ku, Tokyo 113-8657, Japan; [2]JST, CREST, 7, Gobancho, Chiyoda-ku, Tokyo 102-0076, Japan; [3]Research Institute for Bioresources and Biotechnology, Ishikawa Prefectural University, 1-308, Suematsu, Nonoichi, Ishikawa 921-8836, Japan.

Running title: *Tyrosine nitration in rufomycin biosynthesis*

To whom correspondence should be addressed:
Prof. Yasuo Ohnishi, Department of Biotechnology, Graduate School of Agricultural and Life Sciences, The University of Tokyo, 1-1-1, Yayoi, Bunkyo-ku, Tokyo, 113-8657, Japan, Telephone: (+81)-3-5841-5123, FAX: (+81)-3-5841-8021, E-mail: ayasuo@mail.ecc.u-tokyo.ac.jp
Prof. Yohei Katsuyama, Department of Biotechnology, Graduate School of Agricultural and Life Sciences, The University of Tokyo, 1-1-1, Yayoi, Bunkyo-ku, Tokyo, 113-8657, Japan, Telephone: (+81)-3-5841-5124, FAX: (+81)-3-5841-8021, E-mail: aykatsu@mail.ecc.u-tokyo.ac.jp

Keywords: Cytochrome P450, nonribosomal peptide, rufomycin, 3-nitrotyrosine, *Streptomyces*

ABSTRACT

Rufomycin is a circular heptapeptide with anti-mycobacterial activity and is produced by *Streptomyces atratus* ATCC 14046. Its structure contains three non-proteinogenic amino acids, *N*-dimethylallyltryptophan, *trans*-2-crotylglycine, and 3-nitrotyrosine (3NTyr). Although the rufomycin structure was already reported in the 1960s, its biosynthesis, including 3-NTyr generation, remains unclear. To elucidate the rufomycin biosynthetic pathway, we assembled a draft genome sequence of *S. atratus* and identified the rufomycin biosynthetic gene cluster (*ruf* cluster), consisting of 20 ORFs (*rufA*–*rufT*). We found a putative heptamodular nonribosomal peptide synthetase encoded by *rufT*,

a putative tryptophan *N*-dimethylallyltransferase by *rufP*, and a putative trimodular type I polyketide synthase by *rufEF*. Moreover, the *ruf* cluster contains an apparent operon harboring putative cytochrome P450 (*rufO*) and nitric oxide synthase (*rufN*) genes. A similar operon, *txtDE*, is responsible for the formation of 4-nitrotryptophan in thaxtomin biosynthesis; the cytochrome P450 TxtE catalyzes the 4-nitration of Trp. Therefore, we hypothesized that RufO should catalyze the Tyr 3-nitration. Disruption of *rufO* abolished rufomycin production by *S. atratus*, which was restored when 3NTyr was added to the culture medium of the disruptant. Recombinant RufO protein exhibited Tyr 3-nitration activity both *in vitro* and *in vivo*. Spectroscopic analysis further revealed that RufO recognizes Tyr as the substrate with a dissociation constant of ~ 0.1 μM. These results indicate that RufO is an unprecedented cytochrome P450 that catalyzes Tyr nitration. Taken together with the results of an *in silico* analysis of the *ruf* cluster, we propose a rufomycin biosynthetic pathway in *S. atratus*.

Natural products have been found in a wide range of organisms including plants, fungi, microorganisms, and mammals. Because these compounds exhibit various physiological activities applicable to medical and pharmaceutical products, animal drugs, and agricultural chemicals, they have been used to facilitate and improve human life. From a biochemical point of view, these compounds display diverse chemical structures, and many studies have focused on their biosynthetic mechanisms.

The nitro group is not an abundant functional group in natural products, but it has been found in some important bioactive compounds including chloramphenicol, aureothin, and thaxtomin (1,2). Although the mechanism for generating the nitro group in natural products is not fully understood, two possible nitration mechanisms have been reported. One is the oxidation reaction of an amino group found in chloramphenicol, aureothin, and pyrrolnitrin biosynthesis. In the former two cases, the *p*-amino groups of *p*-aminophenylalanine and *p*-aminobenzoic acid are oxidized to *p*-nitro groups using molecular oxygen as a substrate by the non-heme di-iron-containing monooxygenases CmlI (3,4) and AurF (5–7), respectively. In pyrrolnitrin biosynthesis, PrnD, which contains a Rieske iron-sulfur cluster, catalyzes the oxidation of aminopyrrolnitrin to complete the biosynthetic pathway (8). Recently, CreD, a flavin-dependent monooxygenase that is involved in cremeomycin biosynthesis, was reported to catalyze nitro group formation by oxidizing the amino group of Asp (9).

The other mechanism is direct nitration catalyzed by TxtE, a bacterial cytochrome P450 involved in thaxtomin biosynthesis in plant-pathogenic *Streptomyces* strains including

Streptomyces scabies (10–12). TxtE uses nitric oxide (NO) supplied by a nitric oxide synthase (NOS) encoded by *txtD* as its substrate, and it catalyzes the selective nitration of Trp to generate 4-nitrotryptophan. The *txtE* and *txtD* genes are located next to each other, and they form a putative operon in the thaxtomin biosynthetic gene cluster (*txt* cluster) (13).

In addition to these compounds, pyrrolomycins were reported to possess a nitro group in the pyrrole ring (14–18), but the nitration mechanism has not been elucidated in detail (19,20). NOS is not considered to be involved in this mechanism, because NOS inhibitors do not affect the nitration of pyrrole (20). Instead, putative nitrate reductases are encoded by its biosynthetic gene cluster, suggesting that NO is synthesized by the reduction of nitrate (19).

Rufomycin (21,22), also known as ilamycin (23–27), is a circular heptapeptide with anti-mycobacterial activity, which was isolated from *Streptomyces atratus* ATCC 14046. Although its chemical structure was reported in the 1960s (26,27), its biosynthetic mechanisms are unclear. Rufomycin contains three non-proteinogenic amino acids, *N*-dimethylallyltryptophan, *trans*-2-crotylglycine, and 3-nitrotyrosine (3NTyr). The formation of *N*-dimethylallyltryptophan was found in cyclomarin biosynthesis, in which the tryptophan *N*-dimethylallyltransferase CymD catalyzes the *N*-prenylation of free Trp (28,29). In contrast, the mechanisms for generating *trans*-2-crotylglycine and 3NTyr are unknown. Although 2-crotylglycine is an intermediate in the degradation pathway of aromatic rings in *Pseudomonas putida* (30), this pathway is unlikely to be used for 2-crotylglycine synthesis in rufomycin biosynthesis, and no enzymes for 3NTyr formation have been reported. Therefore, elucidating the rufomycin biosynthetic pathway will shed light on novel enzymes involved in the biosynthesis of 2-crotylglycine and 3NTyr.

Here we report the identification and *in silico* characterization of the rufomycin biosynthetic gene cluster (*ruf* cluster). We also report genetic and biochemical analyses of a cytochrome P450 enzyme, RufO, which catalyzes the 3-nitration of Tyr. According to these analyses, we propose a probable rufomycin biosynthetic pathway.

RESULTS

Draft genome analysis of *S. atratus* to identify the *ruf* cluster.

To elucidate the mechanisms of rufomycin biosynthesis and 3NTyr generation, identifying the rufomycin biosynthetic gene cluster is indispensable. Therefore, we first determined a draft genome sequence of *S. atratus* with the HiSeq 2000 system (Illumina) using a paired-end sequencing strategy. Then we searched the draft genome sequence for the rufomycin biosynthetic gene cluster *in silico*. Based on the

rufomycin structure, we assumed that the rufomycin biosynthetic gene cluster should include a nonribosomal peptide synthetase (NRPS) gene(s) for peptide assembly, a tryptophan *N*-dimethylallyltransferase gene for the synthesis of *N*-dimethylallyltryptophan, and a gene(s) for the nitro group synthesis. As expected, we found a gene cluster that satisfied all these requirements (see below) and named it the *ruf* cluster. The nucleotide sequences of partially sequenced regions were determined by primer walking to complete the sequence of the *ruf* cluster (Fig. 1A and Table 1). Twenty ORFs (*rufA–T*) compose the *ruf* cluster, and four of them encode cytochrome P450 enzymes. One of the four cytochrome P450 genes (*rufO*) forms a putative operon with an NOS gene (*rufN*), and these two genes were expected to be responsible for the nitro group synthesis. An NRPS gene (*rufT*) and a tryptophan *N*-dimethylallyltransferase gene (*rufP*) were also found in the *ruf* cluster.

***In silico* analysis of the *ruf* cluster.**

Here we describe the results of our *in silico* analysis of several important enzyme-encoding genes for rufomycin biosynthesis.

(i) NRPS

Because rufomycin harbors three non-proteinogenic amino acids, we assumed that it should be synthesized by an NRPS. In the *ruf* cluster, we found a large gene (*rufT*) encoding a heptamodular NRPS, the domain component of which was consistent with the chemical structure of rufomycin (Fig. 1B). The substrate of each adenylation (A) domain was predicted by NRPS predictor 2 (Table S1) (31,32). Although most of the predictions were not consistent with the structure of rufomycin, the A domain of the loading module was predicted to recognize *N*-dimethylallyltryptophan with high reliability. This result indicates that peptide assembly is initiated from *N*-dimethylallyltryptophan. The location of two methyltransferase (MT) domains at modules 1 and 4 also supports this notion. Modules 1 and 4 correspond to the second and fifth amino acid residues, respectively, in the rufomycin assembly pathway. When *N*-dimethylallyltryptophan is considered to be the first amino acid residue, the second and fifth amino acid residues are both *N*-methylleucine, which agree with the presence of MT domains at modules 1 and 4. Meanwhile, the A domain of module 2 was predicted to incorporate Tyr. This module corresponds to the third amino acid residue of rufomycin, *i.e.,* 3NTyr, assuming *N*-dimethylallyltryptophan is the first amino acid residue. If this prediction is correct, Tyr should be loaded on the thiolation (T) domain of module 2, and 3-nitration should occur during or after peptide assembly. However, because there is no report of A domains recognizing 3NTyr, it is impossible to predict 3NTyr as a substrate of any A domains. Therefore, it is also possible that

3NTy, instead of Tyr, is incorporated to the NRPS.

(ii) Tryptophan *N*-dimethylallyltransferase

In cyclomarin biosynthesis, CymD catalyzes the *N*-dimethylallylation of free Trp (28,29). In the *ruf* cluster, *rufP* encodes a CymD homolog (44% identity). We speculate that *N*-dimethylallyltryptophan is synthesized by RufP.

(iii) Type I polyketide synthase (PKS) for the synthesis of *trans*-2-crotylglycine

PKS genes (*rufE* and *rufF*) were found in the *ruf* cluster. RufE consists of three modules (loading module and modules 1 and 2) and RufF is a thioesterase (TE) (Fig. 2A), and the RufEF PKS is most likely responsible for *trans*-2-crotylglycine biosynthesis. The loading module contains ketosynthase (KS), acyltransferase (AT), and acyl carrier protein (ACP) domains. While KS domains generally catalyze decarboxylative Claisen condensation for C-C bond formation, a group of KSs called KS^Q, in which the Cys residue for substrate binding is substituted by Gln, catalyze only decarboxylation (33). The KS domain of the loading module is classified as KS^Q (Fig. 2B), suggesting that it catalyzes only the decarboxylation of malonyl-CoA to provide the acetyl starter unit. Module 1 consists of KS, AT, dehydratase (DH), ketoreductase (KR), and ACP domains, and module 2 consists of KS, AT, DH, enoylreductase (ER), KR, and ACP domains. RufF is a TE domain. Via such a domain organization, the RufEF PKS is expected to synthesize 4-hexenoic acid (Fig. 2A). In general, the *cis-trans* stereochemistry of a double bond formed by a DH domain can be predicted by analyzing the KR domain of the same module. KR domains can be classified into A, B, and C types based on the presence or absence of the conserved xxD motif and Trp residue, and the stereochemistry of their products can be predicted according to this classification (34). The KR domain of module 1 belongs to the B type, suggesting that the *trans* C=C bond is synthesized by module 1 (Fig. 2C). Thus, we speculate that RufEF produces *trans*-4-hexenoic acid, which is a compatible precursor for *trans*-2-crotylglycine biosynthesis. Hydroxylation and oxidation of the C2 position of *trans*-4-hexenoic acid can form *trans*-2-oxo-4-hexenoic acid, and transamination of the keto group can form *trans*-2-crotylglycine (Fig. 2A). We speculate that these reactions are catalyzed by a cytochrome P450 enzyme (RufC, see below) and an aminotransferase (RufI).

(iv) NOS and cytochrome P450 for the 3-nitration of Tyr

In the thaxtomin biosynthetic gene cluster, *txtD* and *txtE* (encoding NOS and cytochrome P450, respectively) form a putative operon. We also found a putative operon

consisting of NOS, P450, and tryptophan *N*-dimethylallyltransferase genes (*rufN*, *rufO*, and *rufP*, respectively) in the *ruf* cluster. RufO and RufN show 26% and 58% amino acid sequence identities with TxtE and TxtD, respectively. Although the sequence identity between RufO and TxtE was not high, we assumed that RufO and RufN should be responsible for the nitration of Tyr.

(v) Cytochrome P450 monooxygenases

The cytochrome P450 enzymes except for RufO encoded in the *ruf* cluster (RufC, RufM, and RufS) may catalyze occasional oxidative modification reactions, such as the epoxidation of *N*-dimethylallyltryptophan and the hydroxylation and oxidation of Leu, to synthesize other rufomycin derivatives. Although this biosynthetic process is hypothetical, we predict the roles of three P450 monooxygenases. Using a BLAST search with the primary sequence of RufC as query, we discovered several cytochrome P450 monooxygenases (~50% identity with RufC) whose genes form an operon with PKS genes (Fig. S1A). Interestingly, these operons also encode an aminotransferase. In addition, the domain organization of the PKS discovered from *Streptomyces aidingensis* strain CGMCC 4.5739 is identical to that of RufE. Thus, RufC is most likely to be involved in *trans*-2-crotylglycine biosynthesis and this *trans*-2-crotylglycine biosynthesis pathway seems to be distributed to other natural product biosynthetic pathways. Similarly, we predict the functions of RufM and RufS. Among the characterized enzymes, RufM and RufS show the highest identity with CYP107Z4 (46%) and TbtJ1 (45%), respectively. CYP107Z4 and TbtJ1 catalyze the hydroxylation of avermectin to produce 4''-oxo-avermectin (35) and the hydroxylation of Phe or Leu of the thiopeptide thiomuracin (36,37), respectively. This result implies that RufS should catalyze the hydroxylation of Leu; therefore, RufM is considered to play the remaining role, which is epoxidation of the dimethylallyl group.

Gene disruption of *rufO*.

To confirm the involvement of the *ruf* cluster in rufomycin biosynthesis and to examine the contribution of the candidate P450 gene (*rufO*) to 3NTyr synthesis, we disrupted *rufO* using the CRISPR/Cas9 system (38). A disruption plasmid was designed so that the *rufO* coding region should be cut by Cas9 and removed during the repair of the region, guided by the recombination template cassette introduced into the plasmid. After multiple trials, we isolated the *rufO* deletion strain (Δ*rufO*) (Fig. S2).

We cultivated the wild-type and Δ*rufO* strains and compared their metabolic profiles in three nutrient-rich media, Tryptic Soy Broth (TSB), International Streptomyces Project 2 (ISP2), and modified G-2 (MG2). After extracting metabolites with *n*-butanol, the organic phase was

analyzed by LC-MS.

In the wild-type strain cultivated in MG2, we clearly detected the production of four major compounds whose *m/z* values were identical to those of rufomycin derivatives reported previously (Fig. 3 and Table S2) (39). This indicates that these compounds are the rufomycin derivatives. Three of the four congeners (compounds **1**, **2**, and **3** in Fig. 3) were also produced in ISP2 medium, whereas the rufomycin derivatives were hardly produced in TSB (data now shown). In contrast, in the Δ*rufO* strain, we did not detect any rufomycin derivatives or shunt products in any of the media. However, when 3NTyr was added to the culture medium of the Δ*rufO* strain, rufomycin production was fully recovered (Fig. 3). From these results, we conclude that the *ruf* cluster is responsible for rufomycin biosynthesis. In addition, the recovery of rufomycin production in the Δ*rufO* mutant denied the possibility that the mutant lost heptapeptide production because of the unexpected inactivation of *rufP* caused by the possible polar effect of the *rufO* deletion; *rufP* appears to form an operon, *rufNOP*, with *rufN* and *rufO*. Inactivation of *rufP* must inhibit the peptide synthesis, because *rufP* presumably encodes a tryptophan *N*-dimethylallyltransferase essential for producing the first amino acid (*N*-dimethylallyltryptophan) of the rufomycin peptide. We think that the substrate specificity of the A domain in module 2 of the RufT NRPS should be strict and only 3NTyr can be accepted by RufT as the third amino acid residue in the peptide assembly line. Thus, nitration seems to occur prior to peptide assembly.

UV-Vis spectroscopic study of RufO.

To investigate the function of RufO *in vitro*, the recombinant RufO protein with an 8x His-tag at its C-terminus was produced in *Escherichia coli* and purified by nickel chelate affinity chromatography (Fig. 4). The color of the obtained solution ranged from yellow to red, which is typical of cytochrome P450 solutions. The purified RufO protein was subjected to carbon monoxide (CO)-binding and NO-binding spectral analyses (40). Bubbling of CO into the RufO solution resulted in the Soret band shifting from ~ 420 nm to ~ 450 nm (Fig. 5A). In the case of NO, a shift to ~ 440 nm was observed (Fig. 5B). These physicochemical properties are consistent with those of typical P450 enzymes. All these results indicate that the recombinant RufO was purified in an active form.

Substrate-binding analysis of RufO.

The substrate specificity of RufO was examined by investigating substrate-binding spectra (41). We used five compounds: Tyr, Phe, Trp, 4-hydroxyphenylpuruvate (the proximate precursor of Tyr biosynthesis), and 4-aminophenylalanine. The addition of Tyr resulted in the typical type I binding spectra, a

Soret band shift from ~ 420 nm to ~ 390 nm (41), suggesting that Tyr is recognized as a substrate (Fig. 5C). The dissociation constant (K_d) was estimated to be ~ 0.1 μM (Fig. 5D). In contrast, the other four compounds did not give apparent binding spectra, suggesting that they are not recognized as substrates, or that their binding affinity is too low to be detected.

Examination of the enzyme activity of recombinant RufO protein.

To investigate the ability of RufO to nitrate Tyr, we conducted an *in vitro* analysis using the purified RufO protein. Because bacterial cytochrome P450s require a ferredoxin and a ferredoxin reductase as the redox system, putidaredoxin (CamB) and putidaredoxin reductase (CamA), which are involved in camphor biosynthesis in *P. putida* (42), were also prepared as reported previously (Fig. 4). RufO was incubated with Tyr and diethylamine NONOate (DEANO), a chemical NO generator, in the presence of CamA, CamB, and NADH. After incubating the mixtures, the reactions were quenched with HCl and then subjected to an LC-MS analysis. As a result, the formation of 3NTyr was clearly detected, indicating that RufO catalyzes the nitration reaction of free Tyr (Fig. 6). However, regardless of repeated trial and error, we could not increase the amount of 3NTyr produced in this *in vitro* reaction, which hampered the kinetic analysis of RufO (see discussion). We also examined whether Phe, Trp, 4-hydroxyphenylpyruvate and 4-aminophenylalanine could be used as a substrate of RufO in this *in vitro* reaction. Consistent with the results of the substrate-binding spectrum analysis described above, these four compounds were not recognized as a substrate of RufO and no nitrated products were detected (data not shown).

Production of 3-(*N*-acetyl)aminotyrosine by a recombinant *E. coli* strain expressing *rufO* and *camAB*.

To further confirm the Tyr-nitration activity of RufO, we attempted to produce 3NTyr by a recombinant *E. coli* strain. We used a Tyr-overproducing strain AN219 (43) as the host to express *rufO* and *camAB*. The recombinant strain was cultivated and expression of *rufO* and *camAB* was induced, and then DEANO was added to the culture. After a further 24-h incubation, the culture supernatant was analyzed with LC-MS. As a result, 3-(*N*-acetyl)aminotyrosine was detected, indicating that Tyr was converted to 3NTyr by RufO in this strain, because we confirmed that the nitro group of 3NTyr was efficiently reduced and *N*-acetylated to yield 3-(*N*-acetyl)aminotyrosine by the *E. coli* BL21(DE3) resting cells (Fig. S3). In *E. coli*, two major nitroreductases, NfsA and NfsB, were reported to have wide substrate specificity (44), and therefore they may reduce 3NTyr. *E. coli* also has an arylamine *N*-acetyltransferase (45,46), which seems to be

responsible for the acetylation of 3-aminotyrosine. Taken together with the results of all other experiments in this study, we conclude that RufO catalyzes 3-nitration of free Tyr.

DISCUSSION

In this study, we identified the rufomycin biosynthetic gene cluster (*ruf* cluster) in *S. atratus*. Rufomycin harbors a 3NTyr moiety in its structure, and we demonstrated that 3NTyr is synthesized from Tyr by a cytochrome P450 enzyme, RufO.

Based on the bioinformatic analysis of the *ruf* cluster and genetic and biochemical studies of RufO, we propose the biosynthetic pathway of rufomycin as follows (Fig. 7). In the first step, three non-proteinogenic amino acids are synthesized individually. (i) Trp is converted to *N*-dimethylallyltryptophan by RufP. (ii) RufE and RufF, which form a trimodular type I PKS, produce *trans*-4-hexenoic acid. A cytochrome P450 monooxygenase RufC introduces a keto group into the C2 position of *trans*-4-hexenoic acid to generate *trans*-2-oxo-4-hexenoic acid. Finally, a transamination reaction catalyzed by RufI results in *trans*-2-crotylglycine (*trans*-2-amino-4-hexenoic acid). (iii) RufO catalyzes the 3-nitration of Tyr, with NO produced by RufN, to form 3NTyr. In the second step, the heptamodular NRPS RufT assembles seven amino acids using *N*-dimethylallyltryptophan as the first amino acid to synthesize the heptacyclic peptide rufomycin B. During the peptide elongation, two *N*-methyl groups are introduced by the two MT domains located in modules 1 and 4. Of course, further experiments are required to confirm this proposed biosynthetic pathway.

Regarding the proposed biosynthetic pathway for *trans*-2-crotylglycine, a similar pathway has been predicted for the biosynthesis of (4*R*)-4-[(*E*)-2-butenyl]-4-methyl-L-threonine, which is a building block of cyclosporin A (47–49). In this predicted pathway, the polyketide intermediate is hydroxylated by a P450 monooxygenase and further oxidized by a dehydrogenase. However, the *ruf* cluster contains no putative dehydrogenase gene. Therefore, we speculate that the P450 monooxygenase RufC should catalyze two sequential oxidations (hydroxylation and dehydrogenation) to generate the α-keto group, similar to how CYP170A1 catalyzes the two-step oxidation of *epi*-isozizaene to produce albaflavenone in *Streptomyces coelicolor* A3(2) (50).

During rufomycin biosynthesis, the timing of Tyr nitration is of great interest. In the biosynthetic pathway of natural products, many P450 enzymes that catalyze post-assembly reactions (called tailoring reactions) have been reported. In addition, 3NTyr is non-proteinogenic, and it may be toxic to cells. Therefore, nitration of the Tyr residue after peptide assembly was

regarded as reasonable. There was also a possibility that the nitration of Tyr occurs during peptide assembly. For example, Tyr or some intermediate peptides attached to a T domain could be the substrate of the nitration enzyme. However, all our experimental data indicate that 3NTyr is produced from free Tyr and incorporated into the peptide as a substrate of the RufT NRPS. First, the Δ*rufO* mutant produced neither rufomycin nor its denitrated derivatives, and it restored rufomycin production following the exogenous addition of 3NTyr. Second, recombinant RufO catalyzed the nitration of Tyr *in vitro*. Third, 3-(*N*-acetyl)aminotyrosine, the reduced and *N*-acetylated derivative of 3NTyr, was produced by the recombinant *E. coli* cells expressing *rufO* and *camAB*. From these three results, we conclude that Tyr nitration by RufO occurs prior to peptide assembly. It should be noted that no rufomycin derivatives lacking the nitro group on Tyr have been found, although various patterns of modification have been observed within rufomycin (39). This also strongly supports our conclusions that 3NTyr is produced from free Tyr by RufO and that only 3NTyr is incorporated into the peptide assembly by the RufT NRPS because of high substrate specificity of the A domain in module 2.

Many cytochrome P450 enzymes have been studied extensively, but only TxtE and its close homologs were reported to catalyze the direct nitration of aromatic compounds (10–12). The catalytic mechanism of the nitration catalyzed by TxtE was proposed by Barry *et al.* as follows (10). After substrate binding and heme reduction, TxtE combines NO with molecular oxygen to generate a ferric peroxynitrite intermediate, which then undergoes either homolytic cleavage to yield NO_2 and an Fe(IV)=O species (compound II), or heterolytic cleavage initiated by protonation to yield NO_2^+ and an Fe(III)-OH species. In the former case, the nitration of enzyme-bound Trp should occur via NO_2 addition and hydrogen atom abstraction by compound II, resulting in the formation of an Fe(III)-OH species. In the latter case, it should occur via electrophilic aromatic substitution. In both cases, protonation of the Fe(III)-OH species is required for the regeneration of Fe(III)-OH_2 to restore the resting state of the enzyme. Crystal structure analyses of TxtE and an investigation of substrate analogs indicated the substrate recognition mechanisms of TxtE and the substrate properties required for catalysis (11,12). In addition, a recent study discovered that a single mutation of His176 in the F/G loop of TxtE completely shifts the enzyme's regioselectivity from the C4 to the C5 position of Trp (51). The F/G loop is a flexible loop connecting the F and G helices, and it is involved in the open-to-closed transitions of the substrate-binding pocket; His176 also plays a key role in gating these transitions. However, despite these studies, detailed molecular mechanisms of Trp nitration, including the formation of a ferric peroxynitrite intermediate, by

TxtE remain to be elucidated. Moreover, the reason why TxtE does not show conventional monooxygenase activity toward Trp is of great interest. RufO is the first cytochrome P450 revealed to catalyze the nitration of Tyr, and therefore, it will provide new clues to solve the aforementioned issues of nitrating cytochrome P450 enzymes. However, difficulty in the analysis of these nitrating cytochrome P450 enzymes, TxtE and RufO, seems to be ascribed to their low enzymatic activities. No kinetic analysis has been reported for TxtE and we also failed to show enough RufO activity for the kinetic analysis *in vitro*. Therefore, some improvement of the enzyme assay system may be required for further analysis. A fusion protein of TxtE with redox partner proteins was reported to enhance the catalytic efficiency (52).

When we performed a BLAST search using the primary sequence of RufO as a query, we could not find any close homologs with more than 50% amino acid sequence identity in the database. However, we found some uncharacterized RufO homologs whose genes are likely to form an operon with an NOS homolog gene (Fig. S1B). Interestingly, these operons encoding RufO and NOS homologs are located adjacent to NRPS genes. This observation suggests that these RufO homologs should function as aromatic amino acid-nitrating enzymes and be utilized by respective NRPS systems. Studies of these RufO homologs, as well as further structural analyses and mutagenesis studies of RufO, will provide important insights into the mechanisms of the nitration of aromatic compounds, which will extend our knowledge of cytochrome P450 enzymes.

EXPRERIMENTAL PROCEDURES

Strains, media and culture conditions.

S. atratus ATCC 14046 was obtained from the NITE Biological Resource Center (NBRC), Japan, and was cultivated in Mannitol Soya Flour (MS), TSB, ISP2 and modified G-2 (MG2) media. G-2 is a medium optimized for rufomycin production (36). MS medium consists of mannitol (2%) and soya flour (2%). TSB medium consists of tryptic soy broth (3%). ISP2 medium consists of yeast extract (0.4%), malt extract (1%), and glucose (0.4%) (pH 7.2). MG2 medium consists of potato dextrin (5%), glucose (3%), glycerol (1%), molasses (1%), soluble starch (0.5%), soybean meal (0.5%), corn steep liquor (0.5%), $MgSO_4 \cdot 7H_2O$ (0.05%), $CaCO_3$ (0.3%), $Fe(NH_4)_2(SO_4)_2$ (0.01%), $ZnCl_2$ (0.01%), and $MnSO_4$ (0.01%). For solid culture, agar powder (2%) was added to solidify the medium. *E. coli* strains JM109 and ET12567/pUZ8002, used for plasmid construction and conjugation, respectively, were cultivated at 37°C in Luria-Bertani (LB) medium with or without ampicillin (100 mg l^{-1}) and apramycin (50 mg l^{-1}). *E. coli* strains BL21(DE3) and BLR(DE3), used for heterologous gene expression, were cultivated

at various temperature in LB medium or terrific broth (TB). Trace element solution consists of 50 mM $FeCl_3$•$6H_2O$, 20 mM $CaCl_2$•$2H_2O$, 10 mM $MnCl_2$•$4H_2O$, 10 mM $ZnSO_4$•$7H_2O$, 2 mM $CoCl_2$•$6H_2O$, 2 mM $CuCl_2$•$2H_2O$, 2 mM $NiSO_4$•$6H_2O$, 2 mM $NaMoO_4$•$2H_2O$, 2 mM Na_2SeO_3, and 2 mM H_3BO_3. Specific modifications of media are described in respective sections below. Unless mentioned otherwise, all chemicals were purchased from Tokyo Chemical Industry (Tokyo, Japan), Wako Pure Chemicals (Osaka, Japan) or Nacalai Tesque (Kyoto, Japan).

Enzymes and plasmids.

pCRISPomyces-2 (38) was purchased from Addgene (Cambridge, MA, USA). BbsI was purchased from New England Biolabs (Ipswich, MA, USA). Other restriction enzymes and In-Fusion enzymes were purchased from Takara Bio (Shiga, Japan)

Construction of plasmids for *rufO* disruption.

A sequence containing a protospacer and a protospacer adjacent motif (PAM) was chosen in the reverse complementary sequence of *rufO*. Primers containing this sequence, PAM-F/R, (Table S3) were annealed with each other, and the product was introduced into the BbsI site of pCRISPomyces-2, resulting in pCRISPomyces-2/Δ*rufO*-PAM. The approximately 1-kb fragments of the 5'- and 3'-flanking regions of the target sequence to be disrupted were amplified with the primer pairs DrufO5'-F/R and DrufO3'-F/R (Table S3), respectively. After digestion of pCRISPomyces-2/Δ*rufO*-PAM with XbaI, both the amplified fragments were simultaneously introduced into the plasmid using In-Fusion reaction to yield the gene disruption plasmid pCRISPomyces-2/Δ*rufO*.

Disruption of *rufO*.

Transformation of *S. atratus* was carried out by a conjugation method with *E. coli* ET12567/pUZ8002 (53). The *E. coli* cells harboring pCRISPomyces-2/Δ*rufO* were cultivated in LB medium until the OD_{600} reached ~ 0.5. The cells were harvested by centrifugation (5,000 g, for 15 min, at room temperature), washed twice with fresh LB medium and resuspended in fresh LB medium. Spores of *S. atratus* were harvested from the culture on ISP2 solid medium incubated for 7 days at 30°C. The spores were suspended in TSB medium (0.5 ml) and incubated at 50°C for 10 min. The spores and *E. coli* cells were mixed and inoculated on MS solid medium containing $MgCl_2$ (10 mM). After incubation for 16 h at 30°C, the culture was overlaid with sterilized water (1 ml) containing nalidixic acid (0.75 mg) and apramycin (0.75 mg). After a further cultivation for several days, a transformant colony was picked up and inoculated onto ISP2 solid medium. Then, the transformant was repeatedly cultivated on ISP2 solid medium

without apramycin until the cells lost apramycin resistance. Gene disruption was confirmed by PCR using the primer pair DrufO-F/R (Table S3 and Fig. S2).

Comparison of metabolic profiles and rufomycin production.

S. atratus cells were cultivated in TSB, ISP2, and MG2 media at 28°C for 7 days. *n*-Butanol saturated with water was added to the medium at a ratio of 1 : 1 (v/v). The organic layer was concentrated *in vacuo*, and the residual materials were dissolved in methanol and subjected to an LC-electron spray ionization MS (LC-ESIMS) analysis in an 1100 series spectrometer (Agilent Technologies) coupled to high-capacity Trap Plus system (Bruker Daltonics) equipped with a COSMOCORE 2.6 C_{18} column (2.1 ID × 150 mm; Nacalai Tesque, Kyoto, Japan). The compounds were separated with a linear gradient of water and acetonitrile containing formic acid (0.1%) at a flow rate of 0.4 ml min^{-1}.

Production and purification of the recombinant RufO, CamA, and CamB proteins.

The coding region of the *rufO* gene was first amplified from the genomic DNA of *S. atratus* by PCR using the primer pair rufO-F/R (Table S3). During the PCR, an eight-histidine tag-coding sequence was incorporated into the 3' end of *rufO*. pET16b was applied to inverse PCR using the primer pair 16b-inv-F/R (Table S3), and the original N-terminal ten-histidine tag-coding sequence was removed during the PCR. The resultant two fragments were applied to the In-Fusion reaction, and the plasmid obtained (pET16b-*rufO*) was introduced into *E. coli* BLR(DE3) after confirming the absence of unintended mutations. The transformant was cultivated at 37°C in TB with 5-aminolevulinic acid (80 mg l^{-1}), $Fe(NH_4)_2(SO_4)_2$ (40 mg l^{-1}), trace element solution (200 μl l^{-1}), and ampicillin (100 mg l^{-1}) until the OD_{600} reached ~ 0.5. After cooling the medium to room temperature, isopropyl 1-thio-β-D-galactopyranoside (IPTG) was added to a final concentration of 0.1 mM to induce gene expression, and cells were cultivated for a further 20 h at 15°C. Then, cells were harvested, resuspended in lysis buffer (20 mM Tris-HCl (pH 8.0) containing 200 mM NaCl and 10% (v/v) glycerol), and disrupted by sonication. After centrifugation (20,000 g, 20 min, 4°C), His60 Ni Superflow Resin was added to the soluble cell extracts and mixed gently at 4°C for 30 min. After the His-tagged proteins were eluted with lysis buffer containing 0.5 M imidazole, the buffer was exchanged for 25 mM Tris-HCl (pH 8.0) containing 0.1 mM dithiothreitol (DTT) and 0.1 mM ethylenediaminetetraacetic acid (EDTA) using a PD-10 column (GE Healthcare Biosciences).

The pET28b-*camA* and pET28b-*camB*

plasmids (54) were individually introduced into *E. coli* BL21(DE3). The transformants were cultivated at 37°C in LB medium with kanamycin (50 mg ml^{-1}) until the OD_{600} reached ~ 0.5. $FeCl_3$ was added to the culture medium for the *camA* expression at a final concentration of 0.1 mM. After cooling the medium to room temperature, IPTG was added to a final concentration of 0.1 mM to induce expression, and cells were cultivated for a further 12 h at 28°C. Cells were harvested, resuspended in lysis buffer and disrupted by sonication. After centrifugation (20,000 g, 20 min, 4°C), His60 Ni Superflow Resin was added to the soluble cell extracts and mixed gently at 4°C for 30 min. After the His-tagged proteins were eluted with lysis buffer containing 0.5 M imidazole, the buffer was exchanged for 25 mM Tris-HCl (pH 8.0) containing 0.1 mM DTT and 0.1 mM EDTA using a PD-10 column. The protein concentrations were determined using NanoDrop (Thermo Fisher Sceintific) with the millimolar coefficient of 29.1 for RufO, 38.8 for CamA, and 10.3 for CamB.

UV-Vis spectroscopic analysis.

The RufO Fe(II)-CO complex was investigated as follows. The protein solution (5 μM RufO in 25 mM Tris-HCl (pH 8.0) containing 0.1 mM DTT and 0.1 mM EDTA) was prepared, and sodium hydrosulfite (Sigma-Aldrich, St. Louis, MO, USA) was added. The solution was divided into two cuvettes, A and B, and carbon monoxide (CO) gas was bubbled into cuvette A for 2-3 min. UV-Vis spectra of both the cuvettes were measured, and the CO difference spectrum was obtained by the subtraction of the spectrum of cuvette B from that of cuvette A.

The RufO Fe(III)-NO complex was investigated as follows. The protein solution (5 μM RufO in 25 mM Tris-HCl (pH 8.0) containing 0.1 mM DTT and 0.1 mM EDTA) was prepared. Diethylamine NONOate (DEANO) (Sigma-Aldrich) solution was prepared by dissolving DEANO into the same buffer. The protein solution was divided into two cuvettes, A and B. An equivalent volume of the DEANO solution was added to cuvette A, whereas the buffer was added to cuvette B. UV-Vis spectra of both the cuvette were measured, and the NO difference spectrum was obtained by the subtraction of the spectrum of cuvette B from that of cuvette A.

Substrate-binding analysis.

The protein solution (3.4 – 5 μM RufO in 25 mM Tris-HCl (pH 8.0) containing 0.1 mM DTT and 0.1 mM EDTA) was prepared, and divided into two cuvettes, A and B. The potential substrate was added to cuvette A (0.1-5 μM), and the same volume of the buffer was added to cuvette B. The solutions were mixed well. After 2 min, UV-Vis spectra of both the cuvettes were measured. The spectrum of cuvette B was subtracted from that of cuvette A, resulting in the

difference spectrum. For determination of the dissociation constant (K_d) with Tyr, the difference in absorbance of each spectrum at 386 nm and 422 nm was calculated in triplicate, and the average was plotted against the substrate concentration. The K_d value was calculated by fitting the data with a hyperbolic curve.

***In vitro* analysis using the recombinant proteins.**

In vitro enzymatic reaction mixtures contained 3.4 μM recombinant RufO, 1.6 μM recombinant CamA, 3.2 μM recombinant CamB, 1 mM Tyr, 1 mM NADH, and 1 mM DEANO in 25 mM Tris-HCl (pH 8.0) containing 0.1 mM DTT and 0.1 mM EDTA. When the substrate specificity of RufO was examined, Tyr was replaced with Phe, Trp, 4-hydroxyphenylpyruvate, or 4-aminophenylalanine. The reactions were carried out at 28°C for 3 h with reciprocal shaking at 1,500 rpm. After addition of HCl (0.15 M) to the mixtures to solubilize Tyr and 3NTyr and denature proteins, the mixtures were centrifuged (20,000 g, 5 min, room temperature) and applied to LC-ESIMS analysis. The compounds were separated using COSMOSIL 5PYE column (2.0 ID x 150 mm) (Nacalai Tesque) with a linear gradient of water and acetonitrile containing formic acid (0.1%) at a flow rate of 0.4 ml min^{-1}.

Generation of 3NTyr by a recombinant *E. coli* strain expressing *rufO* and *camAB*.

The *camA* and *camB* genes were introduced into pCDFDuet-1. The coding region of *camA* was amplified from pET28b-*camA* by PCR using the primer pair camA-F/R (Table S3). pCDFDuet-1 was applied to inverse PCR using the primer pair pCDFinv-F/R (Table S3). The resultant two amplified fragments were applied to the In-Fusion reaction, resulting in pCDFDuet-1-*camA*. The coding region of *camB* was amplified from pET28b-*camB* by PCR using the primer pair camB-Nde-F/R (Table S3). This fragment and NdeI-digested pCDFDuet-1-*camA* were applied to the In-Fusion reaction, resulting in pCDFDuet-1-*camAB*. After confirming the absence of unintended mutations, pCDFDuet-1-*camAB* and pET16b-*rufO* were introduced together into the Tyr-overproducing *E. coli* strain AN219. The transformant was cultivated at 37°C in TB with 5-aminolevulinic acid (80 mg l^{-1}), $Fe(NH_4)_2(SO_4)_2$ (40 mg l^{-1}), trace element solution (200 μl l^{-1}), ampicillin (100 mg l^{-1}), kanamycin (50 mg l^{-1}), and streptomycin (50 mg l^{-1}) until the OD_{600} reached ~ 0.5. Then, IPTG was added to a final concentration of 0.1 mM to induce gene expression, and cells were cultivated for a further 24 h at 15°C. DEANO was then added to a final concentration of 0.1 mM, and cells were further cultivated for an additional 24 h at 15°C. After centrifugation (20,000 g, 5 min, room temperature) to remove the cells, HCl (0.15 M) was added to the culture supernatant, followed by the second centrifugation (20,000 g, 5 min,

room temperature) to remove the precipitation. The supernatant was analyzed with LC-ESIMS as described above.

ACKNOWLEDGEMENTS

This work was partially supported by CREST, JST (grant number JPMJCR13B3), Japan, Japan Society for the Promotion of Science (JSPS) A3 Foresight Program, Grant-in-Aid for JSPS Research Fellow (grant number 17J06071), and Amano Enzyme Inc., Japan. The *ruf* cluster was deposited to DDBJ under the accession number LC257593. pET28b-*camA* and pET28b-*camB* used for heterologous gene expression were kindly gifted by Dr. Akimasa Miyanaga and Dr. Akira Arisawa.

CONFLICT OF INTEREST

The authors declare that they have no conflicts of interest with the contents of this article.

AUTHOR CONTRIBUTIONS

H.T. designed the study, performed experiments, analyzed data, and wrote the manuscript. Y.K. designed the study, analyzed data, and wrote the manuscript. H.M. contributed to the experiment shown in Fig. S3. Y.O. directed the research, analyzed data, and wrote the manuscript.

REFERENCES

1. Winkler, R., and Hertweck, C. (2007) Biosynthesis of nitro compounds. *ChemBioChem*. **8**, 973–977
2. Parry, R., Nishino, S., and Spain, J. (2011) Naturally-occurring nitro compounds. *Nat. Prod. Rep*. **28**, 152–167
3. Lu, H., Chanco, E., and Zhao, H. (2012) CmlI is an *N*-oxygenase in the biosynthesis of chloramphenicol. *Tetrahedron*. **68**, 7651–7654
4. Knoot, C. J., Kovaleva, E. G., and Lipscomb, J. D. (2016) Crystal structure of CmlI, the arylamine oxygenase from the chloramphenicol biosynthetic pathway. *J. Biol. Inorg. Chem.* **21**, 589–603
5. He, J., and Hertweck, C. (2004) Biosynthetic origin of the rare nitroaryl moiety of the polyketide antibiotic aureothin: involvement of an unprecedented *N*-oxygenase. *J. Am. Chem. Soc.* **126**, 3694–3695
6. Choi, Y. S., Zhang, H., Brunzelle, J. S., Nair, S. K., and Zhao, H. (2008) *In vitro* reconstitution and crystal structure of *p*-aminobenzoate *N*-oxygenase (AurF) involved in aureothin biosynthesis. *PNAS.* **105**, 6858–6863
7. Chanco, E., Choi, Y. S., Sun, N., Vu, M., and Zhao, H. (2014) Characterization of the *N*-oxygenase AurF from *Streptomyces thioletus*. *Bioorg. Med. Chem.* **22**, 5569–5577
8. Lee, J., Simurdiak, M., and Zhao, H. (2005) Reconstitution and characterization of aminopyrrolnitrin oxygenase, a Rieske *N*-oxygenase that catalyzes unusual arylamine oxidation. *J. Biol. Chem.* **280**, 36719–36727
9. Sugai, Y., Katsuyama, Y., and Ohnishi, Y. (2016) A nitrous acid biosynthetic pathway for diazo group formation in bacteria. *Nat. Chem. Biol.* **12**, 73–75
10. Barry, S. M., Kers, J. A., Johnson, E. G., Song, L., Aston, P. R., Patel, B., Krasnoff, S. B., Crane, B. R., Gibson, D. M., Loria, R., and Challis, G. L. (2012) Cytochrome P450–catalyzed L-tryptophan nitration in thaxtomin phytotoxin biosynthesis. *Nat. Chem. Biol.* **8**, 814–816
11. Yu, F., Li, M., Xu, C., Wang, Z., Zhou, H., Yang, M., Chen, Y., Tang, L., and He, J. (2013)

Structural insights into the mechanism for recognizing substrate of the cytochrome P450 enzyme TxtE. *PloS One*. **8**, e81526
12. Dodani, S. C., Cahn, J. K. B., Heinisch, T., Brinkmann-Chen, S., McIntosh, J. A., and Arnold, F. H. (2014) Structural, functional, and spectroscopic characterization of the substrate scope of the novel nitrating cytochrome P450 TxtE. *ChemBioChem*. **15**, 2259–2267
13. Kers, J. A., Cameron, K. D., Joshi, M. V., Bukhalid, R. A., Morello, J. E., Wach, M. J., Gibson, D. M., and Loria, R. (2005) A large, mobile pathogenicity island confers plant pathogenicity on *Streptomyces* species. *Mol. Microbiol.* **55**, 1025–1033
14. Ezaki, N., Shomura, T., Koyama, M., Niwa, T., Kojima, M., Inouye, S., Ito, T., and Niida, T. (1981) New chlorinated nitro-pyrrole antibiotics, pyrrolomycin A and B (SF-2080 A and B). *J. Antibiot. (Tokyo)*. **34**, 1363–1365
15. Ezaki, N., Koyama, M., Shomura, T., Tsuruoka, T., and Inouye, S. (1983) Pyrrolomycins C, D and E, new members of pyrrolomycins. *J. Antibiot. (Tokyo)*. **36**, 1263–1267
16. Koyama, M., Ezaki, N., Tsuruoka, T., and Inouye, S. (1983) Structural studies on pyrrolomycins C, D and E. *J. Antibiot. (Tokyo)*. **36**, 1483–1489
17. Koyama, M., Kodama, Y., Tsuruoka, T., Ezaki, N., Niwa, T., and Inouye, S. (1981) Structure and synthesis of pyrrolomycin A, a chlorinated nitro-pyrrole antibiotic. *J. Antibiot. (Tokyo)*. **34**, 1569–1576
18. Kaneda, M., Nakamura, S., Ezaki, N., and Iitaka, Y. (1981) Structure of pyrrolomycin B, a chlorinated nitro-pyrrole antibiotic. *J. Antibiot. (Tokyo)*. **34**, 1366–1368
19. Zhang, X., and Parry, R. J. (2007) Cloning and characterization of the pyrrolomycin biosynthetic gene clusters from *Actinosporangium vitaminophilum* ATCC 31673 and *Streptomyces* sp. strain UC 11065. *Antimicrob. Agents Chemother.* **51**, 946–957
20. Ratnayake, A. S., Haltli, B., Feng, X., Bernan, V. S., Singh, M. P., He, H., and Carter, G. T. (2008) Investigating the biosynthetic origin of the nitro group in pyrrolomycins. *J. Nat. Prod.* **71**, 1923–1926
21. Fujino, M., Kamiya, T., Iwasaki, H., Ueyanagi, J., and Miyake, A. (1964) Tryptophan moiety of rufomycin homologs. *Chem. Pharm. Bull. (Tokyo)*. **12**, 1390–1392
22. Higashide E. (1968) Studies on Streptomycetes. *J. Agric. Chem. Soc. Jpn.* **42**, 394–400
23. Takita, T., Naganawa, H., Maeda, K., and Umezawa, H. (1964) A new amino acid from ilamycin B1 and the structure of ilamycin B1. *J. Antibiot. (Tokyo)*. **17**, 90–91
24. Takita, T., Naganawa, H., Maeda, K., and Umezawa, H. (1964) Further studies on the tryptophan-parts of ilamycins. *J. Antibiot. (Tokyo)*. **17**, 264–265
25. Takita, T., Ohi, K., Okami, Y., Maeda, K., and Umezawa, H. (1962) New antibiotics, ilamycins. *J. Antibiot. (Tokyo)*. **15**, 46–48
26. Takita, T., Naganawa, H., Maeda, K., and Umezawa, H. (1964) The structures of ilamycin and ilamycin B2. *J. Antibiot. (Tokyo)*. **17**, 129–131
27. Cary, L. W., Takita, T., and Ohnishi, M. (1971) A study of the secondary structure of ilamycin B(1) by 300 MHz proton magnetic resonance. *FEBS Lett.* **17**, 145–148
28. Renner, M. K., Shen, Y.-C., Cheng, X.-C., Jensen, P. R., Frankmoelle, W., Kauffman, C. A., Fenical, W., Lobkovsky, E., and Clardy, J. (1999) Cyclomarins A−C, new antiinflammatory cyclic peptides produced by a marine bacterium (*Streptomyces* sp.). *J. Am. Chem. Soc.* **121**, 11273–11276
29. Schultz, A. W., Lewis, C. A., Luzung, M. R., Baran, P. S., and Moore, B. S. (2010) Functional characterization of the cyclomarin/cyclomarazine prenyltransferase CymD directs the biosynthesis of unnatural cyclic peptides. *J. Nat. Prod.* **73**, 373–377
30. Kunz, D. A., Ribbons, D. W., and Chapman, P. J. (1981) Metabolism of allylglycine and *cis*-crotylglycine by *Pseudomonas putida*(*arvilla*) mt-2 harboring a TOL plasmid. *J. Bacteriol*. **148**, 72–82
31. Röttig, M., Medema, M. H., Blin, K., Weber, T., Rausch, C., and Kohlbacher, O. (2011)

NRPSpredictor2--a web server for predicting NRPS adenylation domain specificity. *Nucl. Acid Res*. **39**, W362–W367
32. Rausch, C. (2005) Specificity prediction of adenylation domains in nonribosomal peptide synthetases (NRPS) using transductive support vector machines (TSVMs). *Nucl. Acid Res.* **33**, 5799–5808
33. Bisang, C., Long, P. F., Cortés, J., Westcott, J., Crosby, J., Matharu, A. L., Cox, R. J., Simpson, T. J., Staunton, J., and Leadlay, P. F. (1999) A chain initiation factor common to both modular and aromatic polyketide synthases. *Nature*. **401**, 502–505
34. Keatinge-Clay, A. T. (2007) A tylosin ketoreductase reveals how chirality is determined in polyketides. *Chem. Biol.* **14**, 898–908
35. Molnár, I., Hill, D. S., Zirkle, R., Hammer, P. E., Gross, F., Buckel, T. G., Jungmann, V., Pachlatko, J. P., and Ligon, J. M. (2005) Biocatalytic conversion of avermectin to 4"-oxo-avermectin: heterologous expression of the ema1 cytochrome P450 monooxygenase. *Appl. Environ. Microbiol.* **71**, 6977-6985
36. Gober, J. G., Ghodge, S. V., Bogart, J. W., Wever, W. J., Watkins, R. R., Brustad, E. M., and Bowers, A. A. (2017) P450-Mediated Non-natural Cyclopropanation of dehydroalanine-containing thiopeptides. *ACS Chem. Biol. In press*
37. Hudson, G. A., Zhang, Z., Tietz, J. I., Mitchell, D. A., and van der Donk, W. A. (2015) *In vitro* biosynthesis of the core scaffold of the thiopeptide thiomuracin. *J. Am. Chem. Soc.* **137**, 16012-16015
38. Cobb, R. E., Wang, Y., and Zhao, H. (2015) High-efficiency multiplex genome editing of *Streptomyces* species using an engineered CRISPR/Cas system. *ACS Synth. Biol.* **4**, 723–728
39. Lambooy, P. K. (2000) Patent WO2000078798 A1
40. Omura, T., and Sato, R. (1964) The carbon monoxide-binding pigment of liver microsomes. II. Solubilization, purification, and properties. *J. Biol. Chem.* **239**, 2379–2385
41. Schenkman, J. B., Remmer, H., and Estabrook, R. W. (1967) Spectral studies of drug interaction with hepatic microsomal cytochrome. *Mol. Pharmacol.* **3**, 113–123
42. Koga, H., Yamaguchi, E., Matsunaga, K., Aramaki, H., and Horiuchi, T. (1989) Cloning and nucleotide sequences of NADH-putidaredoxin reductase gene (*camA*) and putidaredoxin gene (*camB*) involved in cytochrome P-450cam hydroxylase of *Pseudomonas putida*. *J. Biochem. (Tokyo)*. **106**, 831–836
43. Nakagawa, A., Minami, H., Kim, J. S., Koyanagi, T., Katayama, T., Sato, F., and Kumagai, H. (2011) A bacterial platform for fermentative production of plant alkaloids. *Nat. Commun.* **2**, 326
44. Zenno, S., Koike, H., Kumar, A. N., Jayaraman, R., Tanokura, M., and Saigo, K. (1996) Biochemical characterization of NfsA, the *Escherichia coli* major nitroreductase exhibiting a high amino acid sequence homology to Frp, a *Vibrio harveyi* flavin oxidoreductase. *J. Bacteriol.* **178**, 4508-4514
45. Chang, F. C., and Chung, J. G. (1998) Evidence for arylamine *N*-acetyltransferase activity in the *Escherichia coli*. *Curr. Microbiol.* **36**, 125-130
46. Payton, M., Mushtaq, A., Yu, T. W., Wu, L. J., Sinclair, J., and Sim, E. (2001) Eubacterial arylamine *N*-acetyltransferases - identification and comparison of 18 members of the protein family with conserved active site cysteine, histidine and aspartate residues. *Microbiology* **147**, 1137-1147
47. Offenzeller, M., Su, Z., Santer, G., Moser, H., Traber, R., Memmert, K., and Schneider-Scherzer, E. (1993) Biosynthesis of the unusual amino acid (4*R*)-4-[(*E*)-2-butenyl]-4-methyl-L-threonine of cyclosporin A. Identification of 3(*R*)-hydroxy-4(*R*)-methyl-6(*E*)-octenoic acid as a key intermediate by enzymatic *in vitro* synthesis and by *in vivo* labeling techniques. *J. Biol. Chem.* **268**, 26127-26134
48. Walsh, C. T., O'Brien, R. V., and Khosla, C. (2013) Nonproteinogenic amino acid building blocks for nonribosomal peptide and hybrid polyketide scaffolds. *Angew. Chem. Int. Ed. Engl.* **52**, 7098-7124
49. Bushley, K. E., Raja, R., Jaiswal, P., Cumbie, J. S., Nonogaki, M., Boyd, A. E., Owensby, C. A., Knaus, B. J., Elser, J., Miller, D., Di, Y., McPhail, K. L., and Spatafora, J. W. (2013) The genome of

tolypocladium inflatum: evolution, organization, and expression of the cyclosporin biosynthetic gene cluster. *PLoS Genet.* **9**, e1003496

50. Zhao, B., Lin, X., Lei, L., Lamb, D. C., Kelly, S. L., Waterman, M. R., and Cane D. E. (2008) Biosynthesis of the sesquiterpene antibiotic albaflavenone in *Streptomyces coelicolor* A3(2). *J. Biol. Chem.* **283**, 8183-8189
51. Dodani, S. C., Kiss, G., Cahn, J. K. B., Su, Y., Pande, V. S., and Arnold, F. H. (2016) Discovery of a regioselectivity switch in nitrating P450s guided by molecular dynamics simulations and Markov models. *Nat. Chem.* **8**, 419–425
52. Zuo, R., Zhang, Y., Jiang, C., Hackett, J., Loria, R., Bruner, S. D., and Ding, Y. (2017) Engineered P450 biocatalysts show improved activity and regio-promiscuity in aromatic nitration. *Sci. Rep.*, **7**, 842
53. Paranthaman, S., and Dharmalingam, K. (2003) Intergeneric conjugation in *Streptomyces peucetius* and *Streptomyces* sp. strain C5: chromosomal integration and expression of recombinant plasmids carrying the *chiC* gene. *Appl. Environ. Microbiol.* **69**, 84–91
54. Kudo, F., Kawamura, K., Furuya, T., Yamanishi, H., Motegi, A., Komatsubara, A., Numakura, M., Miyanaga, A., and Eguchi, T. (2016) Parallel post-polyketide synthase modification mechanism involved in FD-891 biosynthesis in *Streptomyces graminofaciens* A-8890. *Chembiochem.* **17**, 233–238

TABLES

Table 1. Predicted functions of ORFs in the *ruf* cluster.

ORF	Amino acids	Proposed function
rufA	339	LacI-like regulatory protein
rufB	267	α/β hydrolase
rufC	375	cytochrome P450
rufD	48	hypothetical protein
rufE	4819	type I polyketide synthase
rufF	238	thioesterase
rufG	33	hypothetical protein
rufH	53	MbtH-like protein
rufI	380	aminotransferase
rufJ	135	hypothetical protein
rufK	351	ABC-transporter
rufL	277	ABC-transporter
rufM	402	cytochrome P450
rufN	403	nitric oxide synthase
rufO	394	cytochrome P450
rufP	383	tryptophan *N*-dimethylallyltranferase
rufQ	124	hypothetical protein
rufR	296	luciferase-like monooxygenase
rufS	399	cytochrome P450
rufT	8027	nonribosomal peptide synthetase

FIGURES AND FIGURE LEGENDS

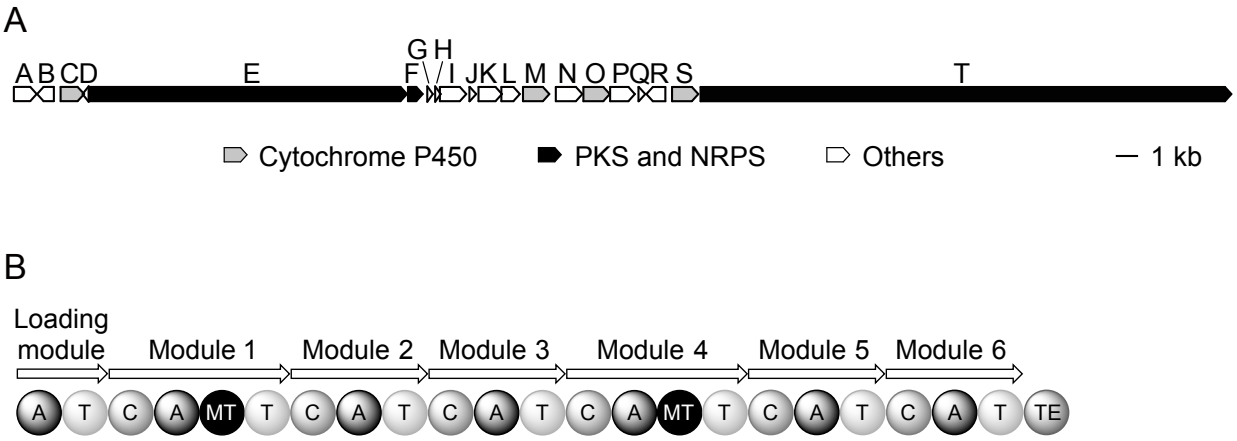

Fig. 1. Gene organization of the *ruf* cluster (A) and domain organization of RufT (B). (A) Genes encoding cytochrome P450 enzymes and PKS/NRPS are colored in gray and black, respectively. Proposed functions of each *ruf* gene product are described in Table 1. (B) A, adenylation domain; T, thiolation domain (peptidyl-carrier protein); C, condensation domain; MT, methylation domain; TE, thioesterase domain.

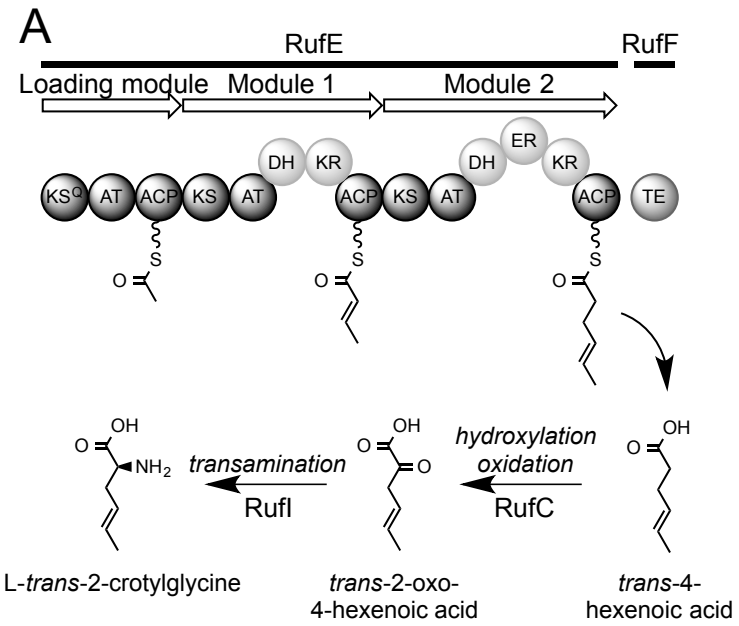

B

```
Nid KSQ VVDTGQSSSLV
Tyl KSQ VVDSAQSASLV
Ery KS1 SVDTACSSSLV
Ruf KSQ TVDTGQASSLA
```

C

```
Ery KR1B ATLDDGT...SSFASAFGA
Ery KR2A GLPQQVA...SSGAGVWGS
Ruf KR1  GIVQDAT...SSASGTLGA
Ruf KR2  GTTRDAA...SSVAGVTGS
```

Fig. 2. Putative pathway for *trans*-2-crotylglycine biosynthesis by the RufEF PKS. (A) *trans*-4-Hexenoic acid is synthetized by the type I PKS consisting of RufE and RufF, and then it is hydroxylated and oxidized by the cytochrome P450 RufC to *trans*-2-oxo-4-hexenoic acid. Finally, *trans*-2-crotylglycine is generated by the transamination catalyzed by RufI. (B) Alignment of partial amino acid sequences of KS and KS^Q domains from type I PKSs. Nid, KS^Q for niddamycin (AF016585); Tyl, KS^Q for tylosin (U78289); Ery, KS1 for erythromycin (X62569); Ruf, KS^Q of the loading module for rufomycin (in this study). The key residue for distinguishing KS and KS^Q is indicated by an *arrow*. (C) Alignment of partial amino acid sequences of KR domains from type I PKSs. Ery KR1B and KR2A, B-type and A-type KRs for erythromycin (L07626 and X62569), respectively; Ruf KR1 and KR2, KRs of module 1 and module 2, respectively, for rufomycin (in this study). The key residues for distinguishing *cis*- and *trans*-type KRs are indicated by *arrows*.

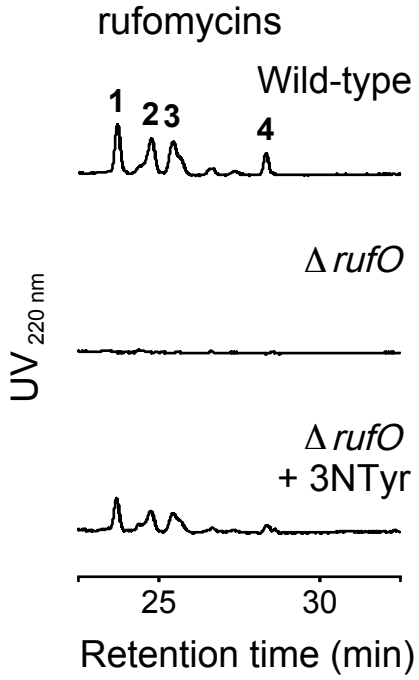

Fig. 3. Metabolic analysis of the Δ*rufO* strain. Compounds were extracted from the whole culture broth using *n*-butanol and separated by reverse-phase liquid chromatography. Four rufomycin congeners (**1**–**4**, see Fig. 7 for their structures) were detected. *Top*, wild-type; *middle*, Δ*rufO*; *bottom*, Δ*rufO* supplemented with 3NTyr.

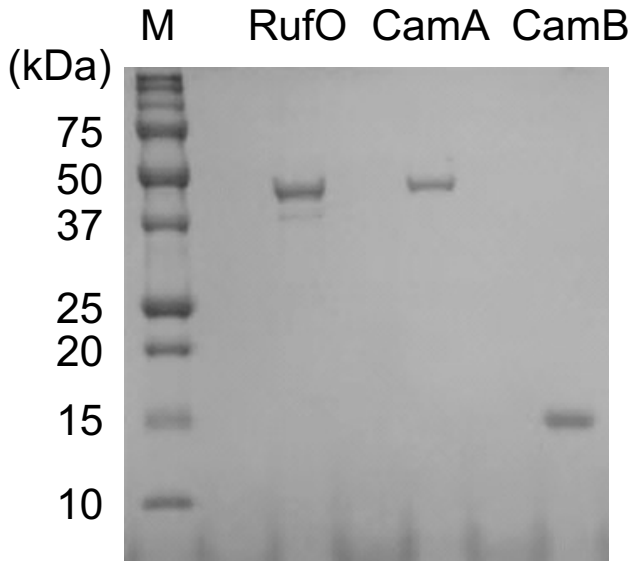

Fig. 4. SDS-PAGE analysis of purified RufO, CamA and CamB proteins. After electrophoresis, the gel was stained with Coomassie Brilliant Blue.

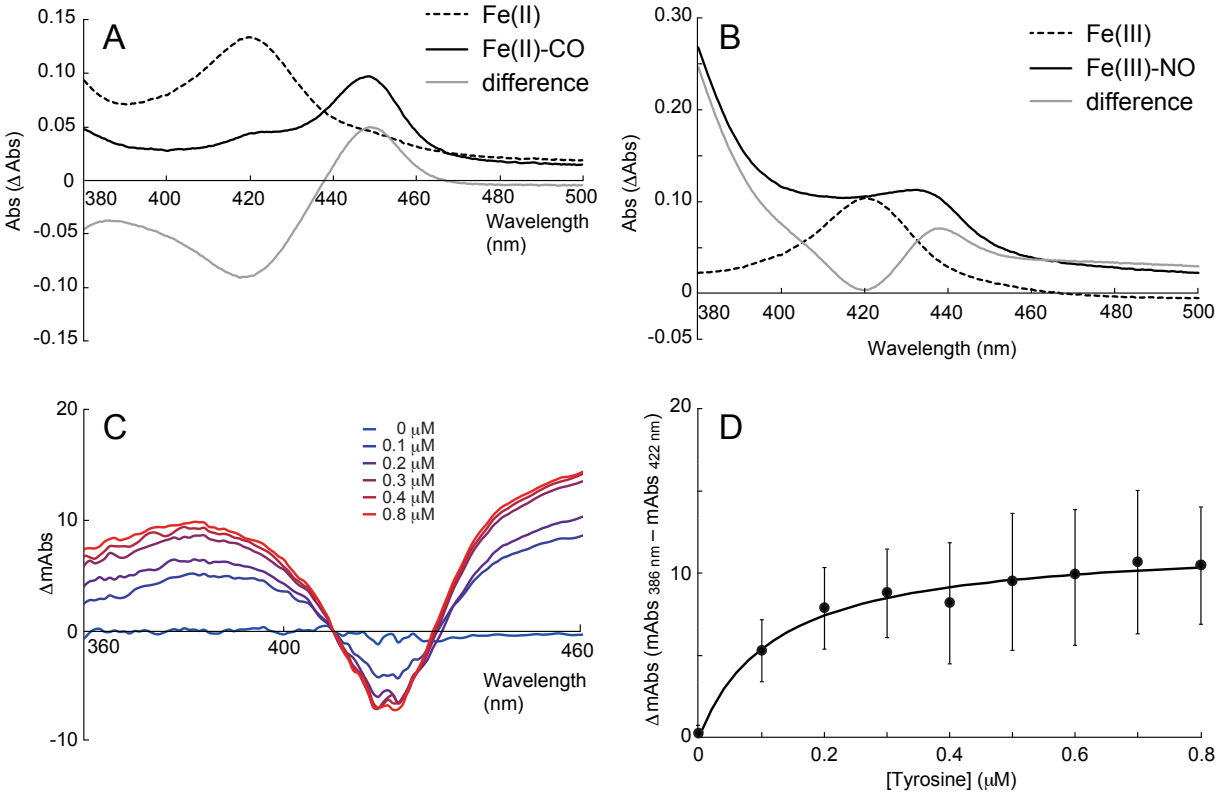

Fig. 5. UV-Vis spectroscopic study on RufO. (A) CO-binding spectra. *Solid line*, RufO with sodium hydrosulfite and CO; *dashed line*, RufO with sodium hydrosulfite without CO; *gray line*, difference spectrum (*solid line – dashed line*). (B) NO-binding spectra. *Solid line*, RufO with NO; *dashed line*, RufO without NO; *gray line*, difference spectrum (*solid line – dashed line*). (C) Tyr-binding analysis. A type I spectral change was observed following the titration of RufO with Tyr (up to 0.8 μM). (D) Difference in absorbance between 386 nm and 422 nm versus the Tyr concentration. The data were fit by a hyperbolic curve, and the dissociation constant was calculated. Assays were conducted in triplicate. *Error bars*, standard deviations.

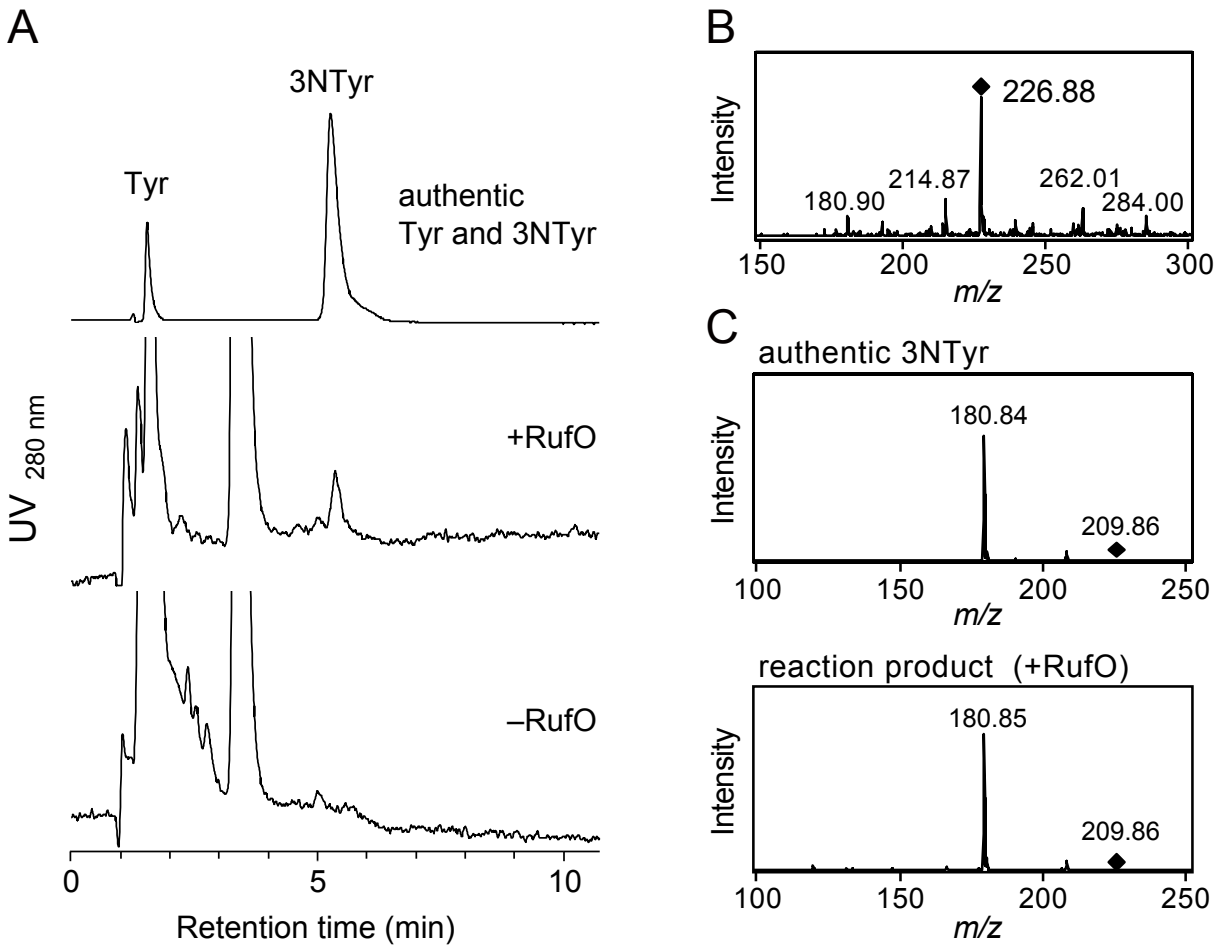

Fig. 6. *In vitro* analysis of RufO. (A) UV chromatogram of the RufO reaction. Compounds were separated by reverse-phase liquid chromatography. *Top*, authentic Tyr and 3NTyr; *middle*, *in vitro* reaction with RufO; *bottom*, *in vitro* reaction without RufO. The sample with enzymes was injected and analyzed prior to that without enzymes and authentic standards. (B) The mass spectrum of the reaction product. 3NTyr (calculated *m/z* ($[M+H]^+$) = 227.1) was clearly detected in the RufO reaction mixture. (C) The tandem mass spectrum of the reaction product was identical with that of authentic 3NTyr.

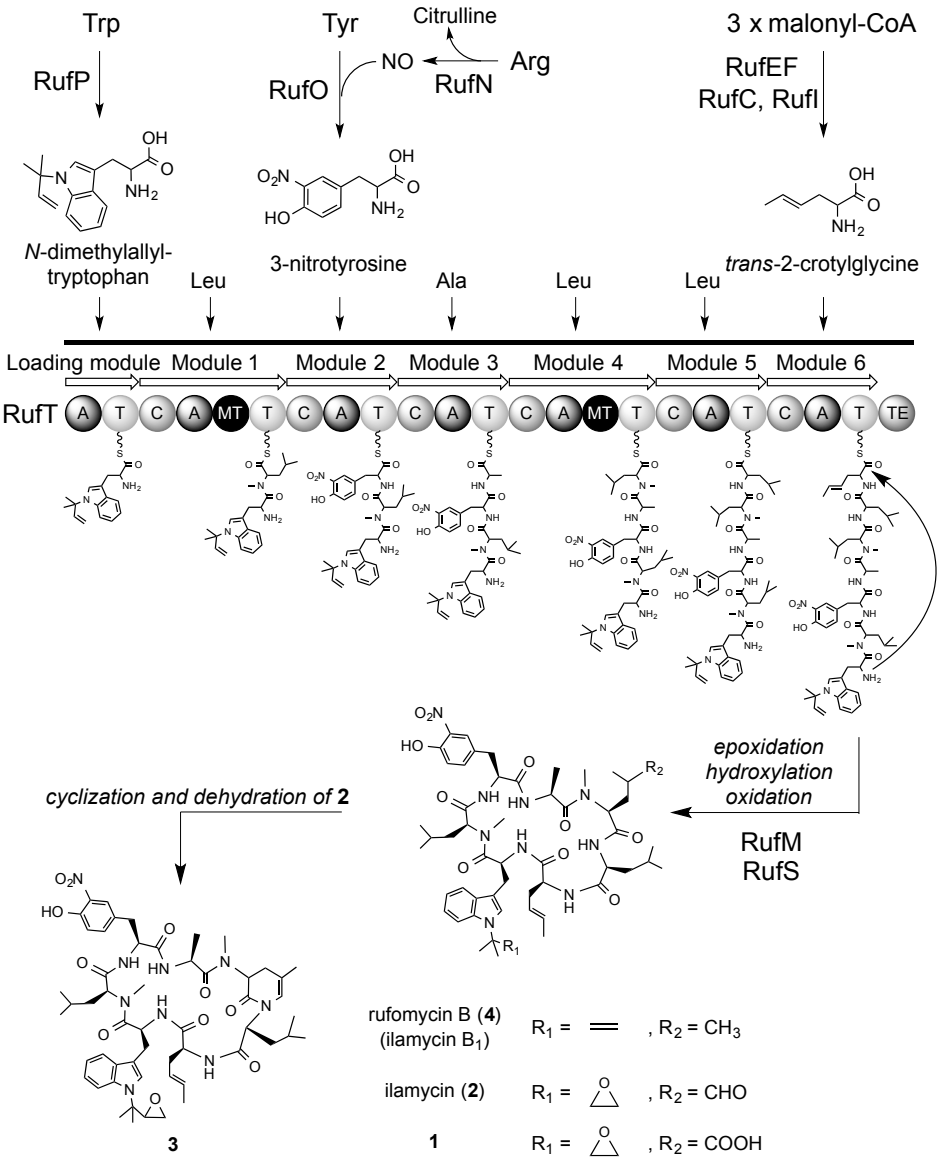

Fig. 7. Proposed pathway for the biosynthesis of rufomycin. Initially, three unusual amino acids, *N*-dimethylallyltryptophan, 3NTyr, and *trans*-2-crotylglycine are synthesized. Subsequently, an NRPS (RufT) assembles seven amino acids using *N*-dimethylallyltryptophan as a starter amino acid, and then the cyclic heptapeptide rufomycin B (**4**) is released. Two cytochrome P450 enzymes modify the peptide occasionally to synthetize other derivatives.

Identification and characterization of a bacterial cytochrome P450 monooxygenase catalyzing the 3-nitration of tyrosine in rufomycin biosynthesis

Hiroya Tomita, Yohei Katsuyama, Hiromichi Minami and Yasuo Ohnishi

J. Biol. Chem. published online August 3, 2017
